[16] Gielis JA. A generic geometric transformation that unifies a wide range of natural and abstratic shapes. *Am J Bot.* 2003;90 (3):333–338.

[17] Wentworth SM. *Fundamentals of Electromagnetics with Engineering Applications*. New York: Wiley; 2005.

[18] Garcia e FCP, Fernandes JM. "Inga," In: Listas de Espécies da Flora do Brasil, Rio de Janeiro, Jardim Botânico do Rio de Janeiro, 2012. http://floradobrasil.jbrj.gov.br/. Access: 10 dez 2016.

How to cite this article: Silva Júnior PF, Freire RCS, Serres AJR, Catunda SY, Silva PHF. Bioinspired transparent antenna for WLAN application in 5 GHz. *Microw Opt Technol Lett*. 2017;59:2879–2884. https://doi.org/10.1002/mop.30853

Received: 14 April 2017

DOI: 10.1002/mop.30850

1.5 μW wake-up-receiver for biotelemetry applications

Sean E. Whitehall | **Carlos E. Saavedra**

Department of Electrical and Computer Engineering, Queen's University, Kingston, Ontario K7L 3N6, Canada

Correspondence
Carlos E. Saavedra, Department of Electrical and Computer Engineering, Queen's University, Kingston, Ontario, K7L 3N6, Canada.
Email: saavedra@queensu.ca

Funding information
This work is funded, in part, by a grant from Natural Sciences and Engineering Research Council of Canada NSERC. Sean Whitehall is the recipient of one NSERC Canadian Graduate Scholarship and three Ontario Graduate scholarships. The circuit was simulated and fabricated using services provided by CMC Microsystems.

Abstract

This article presents a microwave wake-up receiver for biotelemetry applications. The circuit is designed using 130 nm CMOS technology and it consists of a passive amplification front end filter, envelope detector and baseband frequency amplifier with variable feedback filtering. The receiver is designed to operate at 7.6 GHz and measured results show that it has a sensitivity of −40 dBm while drawing just 3 μA from a 0.5 V supply. The presented work has the smallest known area and exhibits a competitive tradeoff between DC power, sensitivity, and bit rate.

KEYWORDS

biotelemetry, CMOS, CMOS RF design, low power RFIC design, wake-up receiver

1 | INTRODUCTION

In the design of microelectronic circuits for wireless body area networks and related biotelemetry applications, minimizing the power consumption is a dominant design constraint. With an ageing population, the demand for such systems is increasing to reduce the cost of monitoring in healthcare.[1] A way to reduce power consumption of the receiver for any device is to duty cycle the receiver, only consuming power when transmission is required. To prevent latency in communication, a separate Wake-up Receiver (WuRx) can be used. This article is about the design and implementation of such a receiver.

Receivers come in two basic architectures; direct detection and super-heterodyne. Direct detection feeds an incident RF signal to a detector at the carrier frequency, usually including a limited amplification stage. Super heterodyne systems use a frequency conversions step to improve amplification and sensitivity, but at the cost of higher circuit complexity and power consumption. The signal is mixed with a Local Oscillator (LO) to produce an intermediate frequency (IF) that is amplified and applied to the detector. The drawback of this approach is that the LO and mixer consume significant dc power, which is inconvenient for biotelemetry systems with very low power constraints.[2,3] The receiver presented here uses direct-detection to eliminate the need for the LO or mixer.

For devices attached to a person, the physical size of devices is of high importance and limits the size of battery that can be used. To eliminate the need for battery replacement of any kind, energy harvesting techniques can be used to sustain indefinite operation. Thermoelectric harvesting converts differences in temperature to electric power and can be applied to a human body. Harvesting energy from human body temperature while restricted to only a few cm^2 struggles to supply more than a few tens of μW.[4–6] Table 1 examines the power consumption of a low power transceiver (2 mW total) when duty cycled with a 2 μW wake-up circuit.

Duty cycle alone does not address the issue of latency, or the time between attempting to communicate and when communication is actually received. To address latency we must examine two varieties of duty cycling, synchronous and asynchronous. Asynchronous communication has lower power consumption, but introduces an undetermined latency between node communication. Synchronous communication requires a wake-up circuit resulting in higher power

TABLE 1 Power consumption of a duty cycled receiver

Duty cycle (%)	0	0.1	1	10	100
DC power (μW)	2	4	22	202	2002

consumption, but reduces the latency in communication. A comparison of asynchronous communication is seen in Figure 1A while Figure 1B shows the latency advantage of a synchronous wake up system.

2 | CIRCUIT DESIGN

The overall circuit in Figure 2 consists an input filter with passive voltage amplification, a detection stage, an IF amplification stage, and comparator. The input capacitor C_{bias} and resistor R_{bias} form a simple High Pass Filter with a lower cut-off of 10^7 Hz. The filter reaches −100 dB at 60 Hz and filters out other low frequency noise from the signal source.

The input match is achieved by an inductor with a resistive impedance of 50 Ohms that is tuned to resonate with the equivalent Capacitance seen at the gate of M_1. The inductor L_r must be tuned to compensate for the loading effect of R_{bias}.

The technology device length is 120 nm and the circuit component values are given in Table 2.

2.1 | Passive gain

The signal is passively amplified using a series LC circuit similar to the one analyzed in [7]. The analysis of the front end is greatly simplified by assuming that C_{bias} and R_{bias} are large enough not to be included in the simplified schematic from Figure 3. The inductor L_r is designed to resonated with the equivalent capacitance C_{eq} representing the gate capacitance of M1, and all parasitic capacitances connected to M1 (node V_g). Assuming the inductor is connected to an RF ground the transfer function input to V_g is

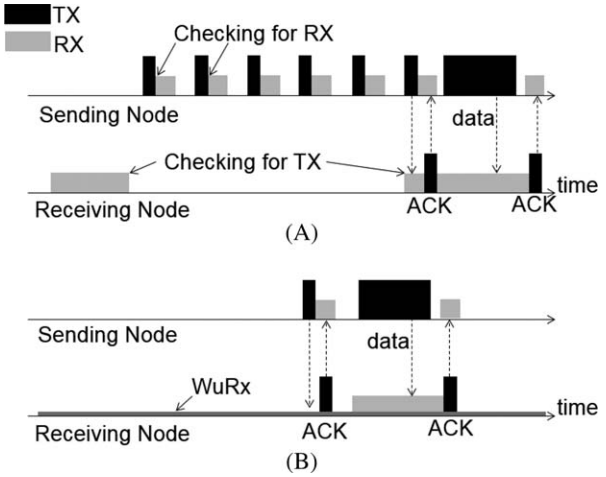

FIGURE 1 Comparison of (A) asynchronous and (B) synchronous duty-cycling

$$\frac{V_g}{V_{in}} = \frac{\frac{1}{j\omega C_{eq}}}{j\omega L_r + R_p + \frac{1}{j\omega C_{eq}}} \tag{1}$$

where L_r is the total series inductance to node V_g and C_{eq} is the equivalent capacitance at node V_g. Inductor L_r is tuned for resonance with C_{eq}, cancelling the reactive components in the denominator to give

$$\frac{V_g}{V_{in}} = \frac{\frac{1}{j\omega C_{eq}}}{R_p} = -\frac{j\omega L_r}{R_p} = -jQ_L \tag{2}$$

where Q_L is the quality factor of Inductor L_r. The gain is typically expressed in dB.

$$A_v = Q_L\left[\frac{V}{V}\right] = 20\log(Q_L)\ [\text{dB}] \tag{3}$$

The resistor R_{bias} is optimized between lower cut-off frequency at the input and degradation of the effective quality factor of the resonance tank. The quality factor of the resonator depends on the inductor L_r and the effective capacitance C_{eq} at the gate of M_1. By keeping $R_{bias} > 5\ k$ the degradation is limited to about 2 dB.

2.2 | Envelope detector

Envelope detection is achieved by applying a high-frequency periodic signal to a non-linear device. The non-linearity results in a baseband output signal to be produced as shown in Figure 4. A common structure for envelope detection is shown in Figure 5. The source follower architecture is used to prevent amplification of RF and baseband noise at the input, leaving the inherent noise of the envelope detector as the dominant source.[2,8,9] In sub-threshold regime, the drain current through M_1 can be expressed as

$$I_d \approx I_{d0} e^{V_{gs}/V_T} \tag{4}$$

where $V_T = nkT/q$ with $1 < n < 2$, k is Boltzmann's constant, T is temperature in Kelvin, and q is the elementary charge. The gate-source voltage across M_1 is given by

$$V_{gs} = V_{RF} + V_{gs0} \tag{5}$$

where V_{RF} is the small RF component and V_{gs0} is the DC component which contributes to the I_{d0} constant in (5). By assuming the DC bias conditions are included in I_{d0} and the RF signal is relatively small, the drain current in (5) can be expanded as

$$I_d = I_{d0} + \frac{dI_d}{dV_{RF}} V_{RF} + \frac{d^2 I_d}{dV_{RF}^2} V_{RF}^2 \tag{6}$$

The second order term from (6) is

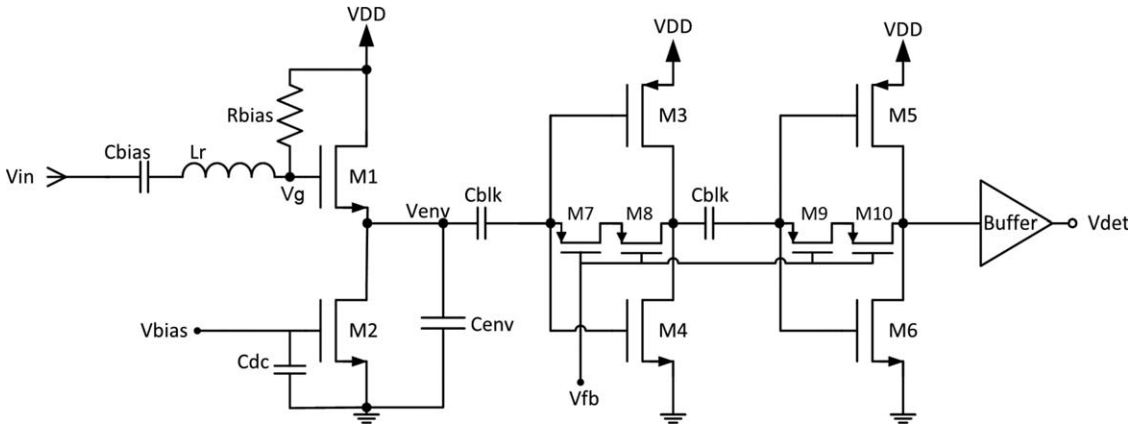

FIGURE 2 The receiver circuit diagram optimized for low space and power consumption for low data rates

TABLE 2 Component parameters for the fabricated circuit

Transistor	M_1, M_2	M_4, M_6	M_3, M_5	M_7, M_8	M_9, M_{10}
Width (_m)	40	10	25	0.4	0.4
Component	C_{bias}	L_r	R_{bias}	C_{blk}	C_{env}
Value (_m)	2 pF	6.9 nH	6 kΩ	3 pF	30 pF

$$\frac{d^2 I_d}{dV_{RF}^2} V_{RF}^2 = I_{d0}/V_T^2. \tag{7}$$

By applying an unmodulated RF signal $V_{RF} = V_s\cos(\omega t)$ the quadratic term above yields $\cos^2(\omega t) = (1 + \cos(2\omega t))/2$. The incremental increase to the baseband output current i_o can be calculated as

$$i_s = I_{d0}\frac{V_s^2}{V_T^2}. \tag{8}$$

It is shown in,[2,8,9] the voltage gain from RF to baseband A_{bb} can similarly be expressed as

$$A_{bb} = \frac{V_s}{4V_T}. \tag{9}$$

At the output, there are three noise sources to consider. First is the thermal noise current contribution from the channel of the transistor M_1 given by

$$i_n^2 = 4\gamma kTg_mB \tag{10}$$

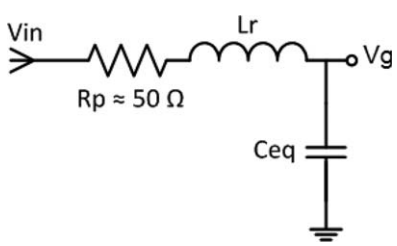

FIGURE 3 Simplified input to demonstrate passive Gain concept

where $g_m = dI_d/dV_g = I_{d0}/V_T$, ≈ 1, and B is the noise bandwidth. From (9) and (10) the output SNR can be given by

$$\text{SNR} = \frac{i_s^2}{i_n^2} = \frac{g_m V_s^4}{64kTV_T^2B} \tag{11}$$

if only thermal noise from M_1 is considered. If $B = gm/2C_{env}$ is substituted into (11) then

$$\text{SNR} = \frac{i_s^2}{i_n^2} = \frac{g_m C_{env}}{10kTV_T^2} \tag{12}$$

shows that a larger capacitor C_{env} directly improves the sensitivity of the detector. To evaluate the match between simple theory and simulation (10) can be modified to

$$v_n^2 = \frac{4\gamma kTB}{g_m} \tag{13}$$

and further to

$$v_n^2 = \frac{2\gamma kT}{\pi C_{env}} \tag{14}$$

The trend is demonstrated through simulation in Figure 6 and shows good agreement between simple theory and computer simulation. The simulation used the full front end of the circuit, but compares favorably to a simulation of the envelope detector in isolation. The slight increase in noise performance is attributed to the passive filtering on the front end of the receiver.

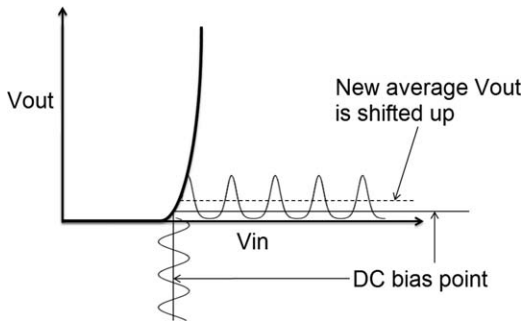

FIGURE 4 The concept of envelope detection of an incident RF signal

The second noise component is baseband noise leakage, which can be kept small by shorting the input signal to ground at the baseband frequencies.[2,8]

The Third component is high frequency interference at the input of M_1, degrading the input signal to noise ratio. When detecting relatively strong signal by wireless communication standards, as wake up receivers typically do, the effect of RF noise around the desired signal is reduced.[2,8,9] The RF noise converted to baseband is analysed and simulated in[8] to conclude it has almost no effect on sensitivity. In[2] experiments are reported to show the same conclusion. The small effect of RF filtering in this work is seen Figure 6 as the difference in noise between the full simulation and isolated envelope detector. In a practical implementation, the receiving antenna would provide more filtering.

The other critical observation from (11) is the performance with respect to the input signal amplitude Vs. Sensitivity depends on input signal amplitude rather than power, allowing passive amplification or voltage transformation to boost performance without the cost of extra DC power.[2,8,9.]

2.3 | IF amplifier

The IF amplifier is designed to eliminate the effect of 1/f noise by reducing the bandwidth of the received bit signal.

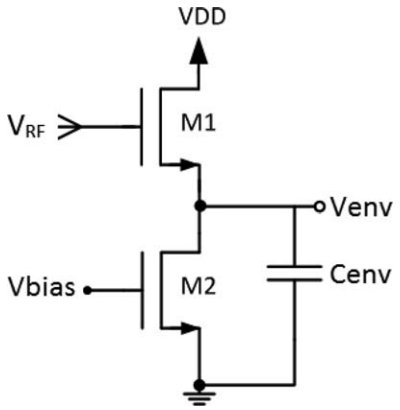

FIGURE 5 A structure for envelope detection used for low noise performance

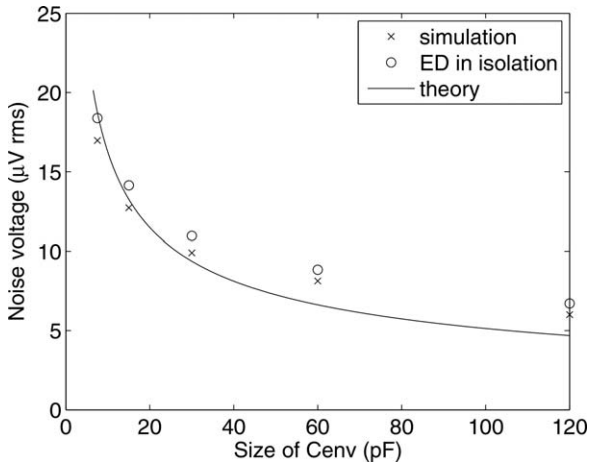

FIGURE 6 Maintaining a constant bandwidth requires power consumption to increase as C_{env} becomes larger

The lower cut of is tunable via feedback voltage V_{fb} to give the linear in dB tuning seen in Figure 7. The feedback resistance is implemented using pfet transistors. Two transistors are used in series to reduce the effect of non-linearity, preventing the circuit behaviour changing for large voltage swings at the output of M_5 and M_6.

Manchester encoding is used to reduce the receiver hardware requirements. In Manchester encoding, bits are represented by transitions between "1"s and "0"s rather than the signal amplitude itself as illustrated in Figure 8. When Manchester encoding is applied, the signal bandwidth shifts upwards, but the spectrum does not increase.[9,10] A 100 kbps signal that is Manchester encoded has information contained between 100 and 200 kHz, allowing the low frequencies to be filtered.

An on-chip buffer is used to drive the oscilloscope and is excluded from the receiver power consumption. The buffer is implemented as a source follower with gain of 0 dB.

3 | MEASUREMENT RESULTS

The circuit was fabricated using the IBM 130 nm CMOS technology, peer reviewed and subsidized by the Canadian

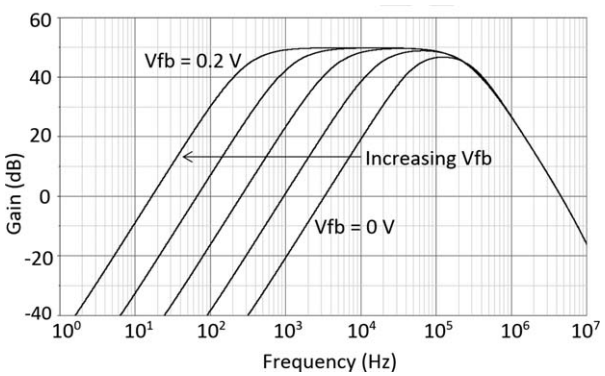

FIGURE 7 IF amplifier can have the lower cut-off tuned using the feedback control voltage V_{fb}

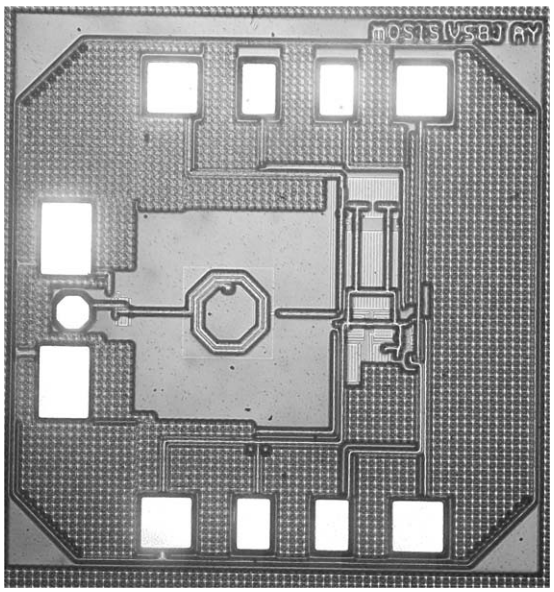

FIGURE 8 Illustration of Manchester encoding example

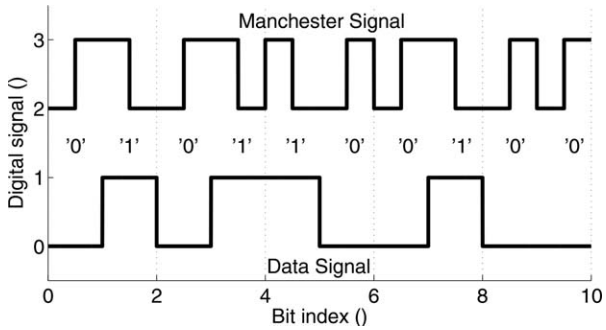

FIGURE 9 Micrograph of the 1 × 1 mm fabricated circuit

Microelectronics Corporation. A photograph of the loose die is seen in Figure 9. The fabricated chip is 1 × 1 mm, but the circuit components occupy just 0.2 mm^2 and the active area for transistors is <0.01 mm^2.

The input reflection coefficient is shifted between simulated and measured results. The simulation was set to 7.7 GHz for compensation but the measured chips consistently match closer to 7.4 GHz. The −15 dB bandwidth is

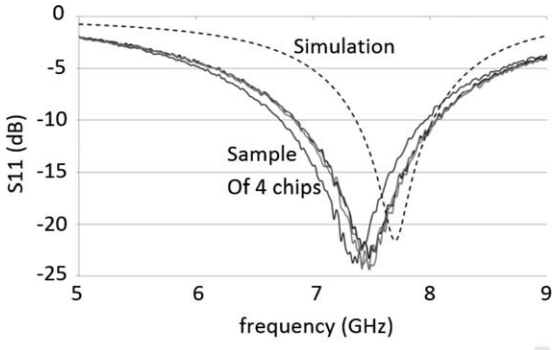

FIGURE 10 Simulated and measured results of input reflection to the circuit

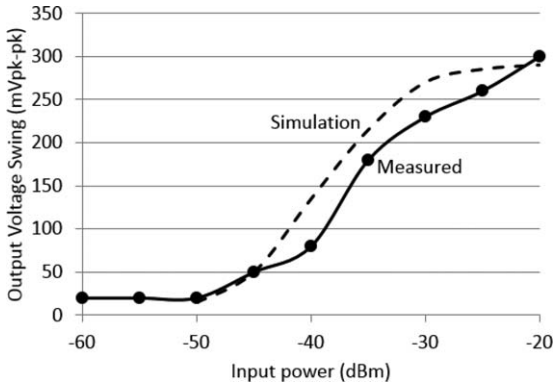

FIGURE 11 Simulated and measured results of output voltage swing when modulated by a 100 kbps OOK signal

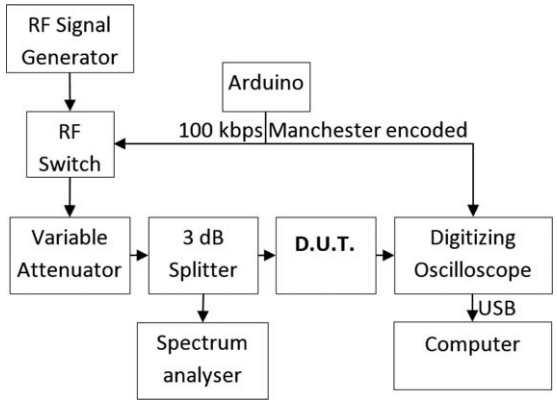

FIGURE 12 Test set up to evaluate the performance of the WuRx

also twice as large for the measured input, suggesting the quality of the resonator is actually less than indicated by the simulation (Figure 10).

When stimulated with an OOK modulated bit steam the receiver generates an output voltage proportional to the input power. The simulated and measured reaction to an input power is shown in Figure 11. Slowing the bit rate to 50 kbps improves the sensitivity to −43 dBm, but increasing to 200 kbps sharply degrades sensitivity to −30 dBm. The upper cut-off frequency of the envelope detector and IF amp are both set to around 200 kHz, so the 400 kHz bandwidth

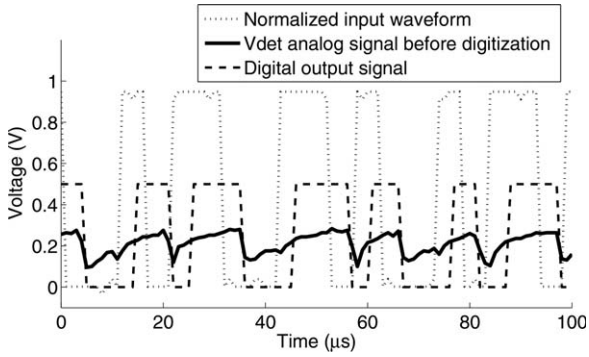

FIGURE 13 Measured input and output waveforms of the circuit during testing, sampled at 1 MHz

TABLE 3 Performance comparison of measured wake-up receivers to date

References	This work	[2]	[11]	[9]	[12]	[13]	[14]
Technology (nm)	130	90	180	130	130	90	65
Carrier (GHz)	7.6	2.4	60	2.4	2.4	2.4	2.4
Supply Voltage (V)	0.5	0.5	1.5	1.0	2.5	1.0	0.5
DC power (μW)	1.5	52	9	2.3	7	10	99
Sensitivity (dBm)	−40	−72	−68[a]	−47	−80	−54	−97
Bit rate (kbps)	100	200	350	100	1	200	10
Total area (mm^2)[b]	0.2	3.0	1.0	105	0.6	0.5	25
Active area (mm^2)	0.009	0.10	0.06	0.007	0.2	0.16	0.06
Year of publication	2016	2009	2013	2013	2015	2016	2016

[a]Actual sensitivity results not obtained, BER is assumed.
[b]Excluding pads.

required for 200 kbps Manchester encoding is not met. The sensitivity is measured in MATLAB from a digitizing oscilloscope sampling the output at 1.0 MHz.

The full test set-up for BER is shown in Figure 12. The RF signal is modulated using an RF switch (Mini Circuits ZYSW-2-50DR) though a variable attenuator to a 3 dB splitter (Mini Circuits ZFSC-2-10G+). The splitter allows the RF power to the circuit to be monitored in real time in parallel with calculation from known attenuation and setting for the RF Signal Generator (Anritsu MG3964A). A sample of a received waveform is shown in Figure 13. The displayed sample is sampled at 1 MHz, and linearly interpolated by MATLAB between the sampled points.

Table 3 contains information from measured wake up receivers to date. The table only considers power consumption below 100 μW with a carrier of at least 1 GHz. The WuRx in[2] is one of the first publications of a sub-100 μW WuRx and is cited by all other works in the table. The WuRx in[9] uses FR4 to set up a transmission line voltage transformer to passively amplify and filter the incoming signal.[12] employs a full super-heterodyne architecture that is duty cycled to reduce data rate and power consumption. References[11,13] both have clock data recovery (CDR) circuits included in the total power consumption. The work presented here offers low power consumption, complexity, and size.

4 | CONCLUSION

Passive amplification can be achieved using very little space and complexity using a single inductor and the parasitic capacitance of a transistor. Die area could be even further reduced if the inductor was simply implemented as a bond wire. As demand for wireless monitoring increases, the low power requirements of individual nodes will continue to tighten and will need to be met with new innovation. The measured circuit uses variable feedback to negate the effect of 1/f noise at baseband frequency.

REFERENCES

[1] Ahn Y, Jayalath D, Oloyede A. A framework for modularised wearable adaptive biofeedback devices. In *2016 IEEE 18th International Conference on e-Health Networking, Applications and Services (Healthcom)*, pp. 1–6, September 2016.

[2] Pletcher NM, Gambini S, Rabaey J. A 52 μw wakeup receiver with −72 dbm sensitivity using an uncertain-if architecture. *IEEE J Solid State Circuits.* 2009;44:269–280.

[3] Thirunarayanan R, Ruffieux D, Enz C. Enabling highly energy efficient wsn through pll-free, fast wakeup radios. In *Circuits and Systems (ISCAS), 2015 IEEE International Symposium on*, pp. 2573– 2576, May 2015.

[4] Abdul Rahman ZH, Khir MHM, Burhanudin ZA, Abdul Rahman AA, Wan Jamil WA. Design of cmos based thermal energy generator for energy harvesting. In *Intelligent and Advanced Systems (ICIAS), 2014 5th International Conference on*, pp. 1–6, June 2014.

[5] Monfray S, Puscasu O, Savelli G, et al. Innovative thermal energy harvesting for zero power electronics. In *Silicon Nanoelectronics Workshop (SNW), 2012 IEEE*, pp. 1–4, June 2012.

[6] Zhang Y, Zhang F, Shakhsheer Y, et al. A batteryless 19 μ w mics/ism-band energy harvesting body sensor node soc for exg applications. *IEEE J Solid-State Circuits.* 2013;48(1):199–213.

[7] Whitehall S, Saavedra CE. A very high-sensitivity cmos power detector for high data rate biotelemetry applications. In *New Circuits and Systems Conference (NEWCAS), 2014 IEEE 12th International*, pp. 145–148, June 2014.

[8] Nilsson E, Svensson C. Envelope detector sensitivity and blocking characteristics. In *2011 20th European Conference on Circuit Theory and Design (ECCTD)*, pp. 773–776, August 2011.

[9] Nilsson E, Svensson C. Ultra low power wake-up radio using envelope detector and transmission line voltage transformer. *IEEE J Emerg Select Top Circ Syst.* 2013;3(1):5–12.

[10]] Elsayed AH, Tadros RN, Ghoneima M, Ismail Y. Low-power all-digital manchester-encoding-based high-speed serdes transceiver for on-chip networks. In *2014 IEEE International Symposium on Circuits and Systems (ISCAS)*, pp. 2752–2755, June 2014.

[11] Wada T, Ikebe M, Sano E. 60-ghz, 9-uw wake-up receiver for short-range wireless communications. In *2013 Proceedings of the ESSCIRC (ESSCIRC)*, pp. 383–386, September 2013.

[12] Milosiu H, Oehler F, Eppel M, Fruehsorger D, Thoenes T. A 7-uw 2.4-ghz wake-up receiver with −80 dbm sensitivity and high co-channel interferer tolerance. In *Wireless Sensors and Sensor Networks (WiSNet), 2015 IEEE Topical Conference on*, pp. 35–37, Jan 2015.

[13] Cheng KW, Lin JS, Chen SE. Reference-less ultra-low-power wake-up receiver with noise suppression. In *2016 URSI Asia-Pacific Radio Science Conference (URSI AP-RASC)*, pp. 994–997, August 2016.

[14] Salazar C, Cathelin A, Kaiser A, Rabaey J. A 2.4 ghz interferer-resilient wake-up receiver using a dual-if multi-stage n-path architecture. *IEEE J Solid State Circuits.* 2016;51(9):2091–2105.

How to cite this article: Whitehall SE, Saavedra CE. 1.5 μW wake-up-receiver for biotelemetry applications. *Microw Opt Technol Lett*. 2017;59:2884–2890. https://doi.org/10.1002/mop.30850

Received: 14 April 2017

DOI: 10.1002/mop.30849

Simplified design, simulation, and lab-environment measurement scheme for retro-directive antenna arrays

Abdul Hannan | **Azhar Hasan** | **Munir Ahmad Tarar**

National University of Science and Technology, Islamabad, Pakistan

Correspondence
Abdul Hannan Munir, National University of Science and Technology, Islamabad, Pakistan.
Email: hannan16800@gmail.com

Abstract

Retro-directive antenna arrays are capable to reflect back an incoming signal in source direction just like corner reflectors. Retro-directive antenna arrays do not use complex and expensive phase shifters or smart antennas to steer their beam. These arrays steer beam autonomously in source direction by reversing progressive phase induced by incident signal. Two basic designs of retro-directive antenna array are Van Atta array and Phase Conjugating array. A simplified design for phase conjugating array is proposed in this article. Moreover, RF measurement and testing in Lab environment need special schemes to cater for issues of multipath, far field reflections, and mutual interference. Therefore, a specially designed lab environment testing methodology is proposed and validation of retro-directive response of developed phase conjugating array using proposed testing methodology is also presented in the article.

KEYWORDS

antenna array, retro-directive, beam steering

1 | INTRODUCTION

Beam forming and beam steering are 2 essentials for RF communication and tracking systems. In recent few years most of RF systems have been developed by using directed beam forming ability for civil and military communication applications. These systems go with smart antenna and phased steering approaches in order to perform functions that require beam forming and beam steering capability. Smart antenna and phased array approach use conventional method of beam steering with help of phase shifters or other complex beam steering methods. These techniques are expensive and complex. In comparison to smart antenna and phased array approaches, retro-directive arrays are of increasing interest because of their simplicity and different functionality.[1]

Retro-directivity is a phenomenon in which a signal is sent back in its source direction without having any previous knowledge about its direction. An antenna array which depicts the phenomena of a retro-directivity is termed as retro-directive antenna array. Retro-directive arrays have the ability to reflect back an incoming signal in source direction. The response is transmitted without any prior knowledge about the location of source and is completely automatic without the use of expensive phase shifters and complex digital circuits autonomous beam steering capability of these arrays makes them a technology of choice for mobile, satellite and back scatter RF communication. It is also used in RF tracking and pointing systems, transponders, UAV command and control systems, microwave beacon and solar power satellites.[2–11] Two basic designs of retro-directive antenna array are Van Atta array and Phase Conjugating array. A